Angry Bird Catapult Dynamics: A parametric study

Submitted by: Divik Bhargava[1], Atharva Shetye[1] and Philip Ng[1]

***Abstract*— This project investigates the dynamics of an elastic slender metal beam used as a catapult to launch a red bird, focusing on the effects of the release angle and material properties on the bird's range. Employing an energy conservation approach, the system's total internal energy is analyzed and discretized, enabling the implicit estimation of the bird's trajectory as it follows a projectile path. By varying the release angles, the study determines the angle that yields the maximum range, the primary objective of the first part. The investigation also explores how changes in material elasticity, and beam slenderness ratio impacts the bird's range. An extension to the first part, a Y shaped catapult is modeled to replicate a sling which would be used to project the bird in the air just like in the game of 'Angry Birds'. In the second part, an inverse approach is taken, using desired range and energy as inputs to calculate the optimal release angle. This research builds upon historical knowledge of catapults and leverages insights from video game physics and elastic systems modeling to create a comprehensive framework for understanding and optimizing the bird's flight.**

I. Introduction

Dating back to 400 B.C, the catapult is a powerful ancient projectile launching mechanism. Traditionally, catapults are built using a rigid frame, arm, tensioning rope, and pivot. Potential energy is stored in the tensioning rope then, via a quick release system, is transformed into kinetic energy at the pivot. This causes a powerful moment on the arm, which rotates the arm rapidly. The kinetic energy of the arm is then transferred to the projectile. Albeit a simple mechanism, there are many moving parts. Using elastic materials, we can minimize the number of parts required; one elastic "beam" arm can retain and convert potential energy. Extensive research has been conducted on the simple catapult mechanism, as well as elastic alternatives. First we will focus on literature on the simple mechanism, then extend this knowledge to literature on elastic systems.

The simple catapult mechanism and design was studied from an experimental level [1]. Researchers from the Echelon Institute of Technology developed a design for a small catapult and retrieved empirical data on the relationship between the distance and back angle of the catapult (the angle at which the catapult arm is released). The researchers chose an arm length of 550mm and obtained the following results 1.

Back angles past 75 degrees were not tested due to limitations of the catapult design. One can observe a nonlinear, increasing relationship between distance and back angle. Although this review does not offer an analytical relationship, it can help us better understand how the projectile will travel, allowing for higher accuracy. It also provides information on constructing a base for the catapult, which is irrelevant to the simulation but relevant for fabrication and testing of a future elastic design.

Angle(θ)	Distance (m) Trials				Arm lengt	Average distance
	D1	D2	D3	D4		
63	9.8	10	10.2	9.8	550	10
53	6.8	7.0	7.2	7.0	550	7
43	3.3	3.2	3.7	3.6	550	3.5
33	2.2	2.0	1.8	2.0	550	2
23	1.5	1	0.8	0.7	550	1
13	0.4	0.6	0.3	0.3	550	0.4

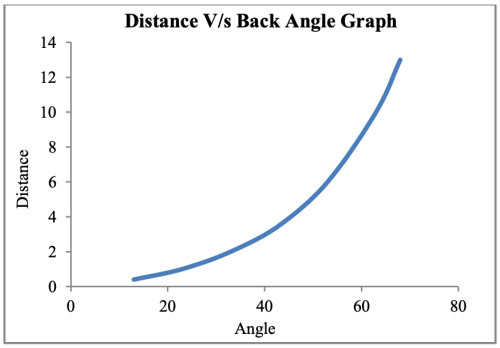

Fig. 1. Distance vs Back angle (Armanini, C., et al) [1]

Unsurprisingly, research into video game physics offers valuable insight for the simulation of a catapult. In his report, "Physics for Game Programmers", researcher Grant Palmer outlines the governing kinematics equations for projectile motion, as well as more complex concepts like conservation of energy, linear momentum and collisions. These concepts will be useful in determining the trajectory of projectile motion, as well as determining how much force transfers from the catapult arm to the projectile.

Methodology for modeling elastic members are discussed further in "Unifying Rigid and Soft Bodies Representation: The Sulfur Physics Engine" [2]. This game physics engine utilizes nodes and edges, approximated as bending springs, to simulate complex elastic geometries. Additional concepts, such as Rayleigh spring damping, are also taken into account. This not only makes the simulation more realistic, but mitigates oscillations and vibrations that could destabilize the simulation. Figure 2 is an example of soft and rigid bodies simulated in the Sulfur Physics Engine.

Extensive research has also been conducted on elastic catapult designs [3]. A study from the University of Trento, describes an experimental setup involving an elastic rod clamped at one end and a load attached to the other end. When the load is smaller than the buckling value, the rod

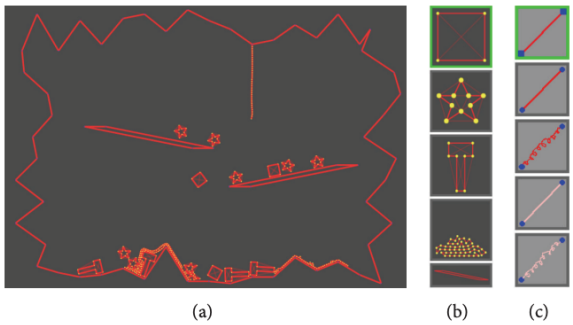

FIGURE 9: Soft and rigid bodies in SulfurChamber.

Fig. 2. Soft and rigid bodies in Sulfur Physics Engine, which closely resemble the skeleton of our system [2]

forms various shapes, creating a closed curve resembling a circle if the rod were rigid. However, the simulation is calculated using Euler elastic theory, or Elastica Theory. For higher loads, the rod reaches a critical configuration, leading to a snap-back instability resembling an "elastica catapult." The entire process, including the critical configuration, is calculated using elastica and simulated using numerical methods from FEA software. To generate our own solution, we must look to literature on Discrete Elastic Beams [4].

A. Problem Definition

There is an elastic slender metal beam with its one end fixed. The other end is bent to a certain position and the red bird is placed on the free end. This system is released in this state for the bird to follow a projectile motion. At the time of release there is a certain angle made by the tangent of the last node with the origin which has an effect on the range of the ball. We have to study the effects of this angle on the range of the bird and therefore calculate the maximum range this bird can get from the designed system. Besides angle, we have to take into the account the material properties of the beam as well for its effects on the range. For this problem, we will limit the number of materials to 3. Also, we will look how the geometry parameters such as slenderness ratio affects the overall projectile. As an extension to the part 1, we modeled a Y catapult fixed at bottom and an elastic string which when stretched at an angle and released projects the bird to follow projectile motion.

The second part of the problem is an inverse approach to the first one. Given the desired range, we have to calculate the angle at which the bird can be projected.

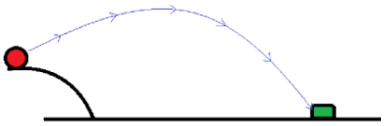

Fig. 3. System representation

II. Methodology

This given problem can have numerous approaches to solve but for this particular project we are using the energy conservation approach. We are keeping the total energy of the system constant at any given time point. Initially, when the beam is bent to a certain angle, it stores the internal elastic energy within itself. We calculate this energy at this point which we are calling Total Internal Energy (E). The red bird, of negligible mass compared to the metal beam, is placed on the very last node of the beam just at the time of release. When the beam is released, its total internal energy will be converted into kinetic energy of the bird thus making it follow a projectile path. Therefore, we will discretize E and solve it implicitly to estimate the trajectory of the bird. Through this trajectory we would then calculate the range of the bird's flight. We run the simulation for different release angles and assess which angle gives the maximum range, which is the desired outcome of part 1 of the problem. Having known all the inputs and variables, we would change the constants like elasticity of the beam to understand the effect of material on the range of the bird.

For part 2 of the problem, we have to take an inverse approach wherein we feed in the range and energy to the simulation to calculate the release angle. Firstly, we record coordinates of the desired range and also calculate the total energy required for the bird to land on that specific location. These will act as inputs to the simulation which will help us in calculating the release angle of the bird

A. Simple Catapult Modeling

For the first part of the project, we created a model in MATLAB that simulates a simple catapult. This was achieved by simplifying the catapult design as a slender beam with a clamped boundary condition. This initial iteration forms a proof of concept for a much complex Y beam catapult, which is discussed in the later section.

1) Model Setup: In this simulation, we approximated the catapult as a 2-D beam composed of $N = 50$ nodes strung together by edges acting as stretching and bending "springs." The $N = 50$ nodes in the beam each have equal mass and are approximated as infinitesimal rectangular prisms with width 3cm and 3.5mm. We chose the simulation to have a duration of 3 seconds, and a `dt` of 0.01s.

The physical parameters were also fixed. The mass of the bird was fixed to $m = 0.01kg$. The density of the rod was

7500 kg/m^3, and the elastic modulus of the beam was set to 200GPa, in the range of metals. The moment of inertia I, was also fixed, as the width, length and thickness of the beam are fixed.

With the physical and simulation parameters defined, we defined the DOF vector for the catapult. Since the current problem is in 2-D, we can set up the following N-DOF vector, **q**:

$$\mathbf{q} = \begin{bmatrix} x_1 \\ y_1 \\ x_2 \\ y_2 \\ \vdots \\ x_a \\ y_a \end{bmatrix}$$

$2N \times 1$ vectors for stretching and bending energies were also initialized. The free DOFs were defined as every node except the first two nodes, which are fixed by a clamped boundary condition.

2) Equations of Motion: In this section, we introduce the physical equations required to simulate the beam in 2-D.

$$\frac{m_i}{\Delta t^2}[\frac{q_i(t_{k+1} - q_i(t_k)}{\Delta t} - \dot{q}_i(t_k)] +$$

$$\frac{\partial E_{potential}}{\partial q_i} + c_i[\frac{q_i(t_{k+1} - q_i(t_k)}{\Delta t}] + W = 0 \qquad (3)$$

This is the discretized, implicit equation of motion for the beam, taking into account the weight of the beam without additional external forces. The elastic potential energy $E_{potential}$ is given by the summation of the stretching and bending energies:

$$E_{potential} = \sum_{a=1}^{n} E_a^s + \sum_{e=1}^{n} E_b^b e \qquad (4)$$

where a is the number of nodes and e is the number of edges. In order to calculate the gradient of the elastic potential energy $\frac{\partial E_{potential}}{\partial q_i}$, we must use the following use the `gradES` and `gradEb` functions[5].

Next, we must calculate the total force of the system **f** and its Jacobian **J**. With the mass, damping, and DOF vector defined, the governing force equation (1) becomes

$$\boldsymbol{f} = \boldsymbol{M}\ddot{\boldsymbol{q}} + \frac{\partial E_{potential}}{\partial \boldsymbol{q}} + \boldsymbol{C}\dot{\boldsymbol{q}} + \boldsymbol{W} = 0 \qquad (5)$$

To solve (5) implicitly, Newton Rhapson Iteration, must be used, which further requires calculation of the Jacobian. The Jacobian is the gradient of the force equation, which yields the discretized equation

$$\boldsymbol{J} = \frac{\boldsymbol{M}}{\Delta t^2} + \frac{\boldsymbol{C}}{\Delta t} + \frac{\partial^2 E_{potential}}{\partial^2 \boldsymbol{q}} \qquad (6)$$

where

$$\frac{\partial^2 E_{potential}}{\partial^2 \boldsymbol{q}} = \sum_{i}^{n} \frac{\partial^2 E_i^s}{\partial^2 \boldsymbol{q}} + \sum_{i}^{n} \frac{\partial^2 E_j^b}{\partial^2 \boldsymbol{q}} \qquad (7)$$

For the Jacobian only, the Hessians of stretching and bending energy can be calculated using `hessEs` and `hessEb`, respectively[5].

3) Implicit Method Iteration: To begin the time-stepping process, we set the timestep to $dt = 10^{-2}$ seconds, an ending time `maxTime` $= 3$, and a variable measuring the number of time steps `steps = round(maxTime / dt)`. Finally, we set a force-dependent tolerance `eps = E*I/l^2 * 1e-3` for the Newton-Rhapson method and an initial error `err = 10 * eps`. Now we can proceed with the time-marching scheme.

The pseudocode for the Newton-Rhapson iteration is as follows:

Algorithm 1 Implicit Iteration via Newton-Rhapson

```
for every timestep from 0 to endtime do
    Update old DOFs and velocities
    Redefine error
    while error > tolerance do
        Define function f without elastic energy
        Define Jacobian J without elastic energy
        Update gradient and Jacobian of linear springs
        for all DOFs do
            get gradients using gradEs and hessEs
            Add results of gradEs to f
            Add results of hessEs to J
        end for
        Update gradient and Jacobian of bending springs
        for all DOFs do
            get gradients using gradEb and hessEb
            Add results of gradEb to f
            Add results of hessEb to J
        end for
        Update DOF vector and error
        Update q: q = q − J^−1 f
        Update error: err = absolute sum of f
        Update middle node velocity
    end while
    Store new DOF vector and velocities
    plot the beam positions in real time
end for
```

Because the results of `hessES` and `gradES` are 4 X 4 matrices, they can only take four DOF components as parameters. To ensure proper matrix addition, we use the following indices:

```
f(2*i-1:2*i+2) = f(2*i-1:2*i+2)
+ dF; J(2*i-1:2*i+2,2*i-1:2*i+2) =
J(2*i-1:2*i+2,2*i-1:2*i+2) + dJ;
```

For `hessES` and `gradES`, which are 6 X 6 matrices, we choose these six DOF components as parameters:

```
  f(2*i-3:2*i+2) = f(2*i-3:2*i+2)
+ dF; J(2*i-3:2*i+2,2*i-3:2*i+2) =
J(2*i-3:2*i+2,2*i-3:2*i+2) + dJ;
```

A similar iteration process is used in the following 3D case.

B. Y Catapult Modeling in 3D plane

After gaining confidence in the initial design and successfully modeling the projectile motion of the bird, our focus shifted to modeling the catapult as a network of beams forming a Y shape. This design posed several challenges, particularly in managing the arrangement of multiple beams. Special attention was devoted to accurately modeling the joints. The system comprises three beams, all sharing the same material and dimensional properties. The vertical beam is clamped at the bottom, and all three beams are connected at Joint 1.

An additional beam, modeled as an elastic string, connects the inclined beams of the Y system. This connection forms Joint 2 and Joint 3 with the left and right inclined beams, respectively. This beam is intended to flex in YZ plane, contributing to the overall elastic energy of the system and propelling the bird.

1) Model Setup: Each inclined beam in the Y system has a length of 60 cm and forms an angle of α when considered together. The vertical beam, originating from the origin, has a length of 50 cm. All beams share a common circular cross-section with outer and inner radii denoted as R_{out} and R_{in}, respectively, both set to 5 mm and 3 mm. The elastic modulus for these beams is defined as 5 GPa, which represent wood.

The string on the other hand is modeled as a flexible beam, with an elastic modulus of 0.005 GPa and a radius of 5mm. The DOF vector q for the complete system is shown below:

$$\begin{bmatrix} \boxed{x_{1,L}} \\ \boxed{y_{1,L}} \\ \boxed{z_{1,L}} \\ \vdots \\ x_{n,L} \\ y_{n,L} \\ z_{n,L} \\ \\ \boxed{x_{1,R}} \\ \boxed{y_{1,R}} \\ \boxed{z_{1,R}} \\ \vdots \\ x_{n,R} \\ y_{n,R} \\ z_{n,R} \end{bmatrix}$$

$$\begin{bmatrix} \boxed{x_{1,V}} \\ \boxed{y_{1,V}} \\ \boxed{z_{1,V}} \\ \vdots \\ x_{n,V} \\ y_{n,V} \\ z_{n,V} \\ \\ x_{1,S} \\ y_{1,S} \\ z_{1,S} \\ \vdots \\ x_{n,S} \\ y_{n,S} \\ z_{n,S} \end{bmatrix}$$

2) Estimation of Forces and their gradient: An initial displacement is applied at the center node of the string, causing it to stretch in the -Y and -Z directions by 30 mm each. This induces the accumulation of stretching energy within the entire system, as the stretched string exerts a force on the Y-shaped structure, leading to effective bending. The stretching forces are determined by calculating the gradient of stretching energy between two consecutive nodes.

Simultaneously, the bending forces are computed by evaluating the gradient of bending energy at each node, involving three consecutive nodes. The Hessians of bending and stretching energy are utilized to calculate the Jacobian of the equation of motion. This comprehensive approach allows for the accurate modeling of both stretching and bending behaviors in the system.

3) Treatment of Joints: Special attention was dedicated to identifying additional bending forces at joints J1, J2, and J3. For joint J1, three specific combinations of bending were taken into account: between the second node of the left and right beams, the left and vertical beams, and the right and vertical beams. The total bending forces at Joint J1 result from the summation of all potential bending forces between inter- and intra-connected nodes. The Jacobian matrix is then updated to incorporate the cumulative Hessian of these bending forces. Similarly, the bending energy and Hessian are computed for all participating nodes that form joints J2 and J3. This comprehensive analysis ensures a thorough consideration of bending effects at each joint, contributing to a more accurate representation of the overall system behavior.

It is important to note that the joint coordinates appears more than once in the DOF vector. For instance, the first coordinates of each Y beam represents the coordinate of J1. Similarly, J2 and J3 have two occurrence each, as the joint is shared between two beams. Forces and their Jacobian are summed and equated for all the coordinates that represent a particular joint.

4) Equation of motion: The equation of motion captures the comprehensive interplay of internal and external forces

acting on each node within the system. This dynamic equation meticulously accounts for stretching forces, bending forces, and the omnipresent gravitational force. It is crucial to emphasize that the gravitational force specifically operates in the -Z direction, and consequently, its inclusion is limited to the computation of forces in the Z direction. The discretized manifestation of this intricate equation is delineated in the form of equation (9). This discretization process ensures that the continuous forces and interactions are effectively represented within a discrete framework, allowing for numerical analysis and simulation. Simultaneously, the potential energy, denoted by E, is a key element in this formulation. Equation (10) encapsulates the essence of potential energy within the system, which is the sum total of bending and stretching energy. These equations are the same as the previous 2-D case.

$$f = m_i \ddot{q}_i + \frac{\partial E_{potential}}{\partial q_i} + c_i \dot{q}_i + W = 0 \tag{8}$$

The discretized equation of motion is as follows.

$$\frac{m_i}{\Delta t^2}[\frac{q_i(t_{k+1} - q_i(t_k)}{\Delta t} - \dot{q}_i(t_k)] +$$

$$\frac{\partial E_{potential}}{\partial q_i} + c_i[\frac{q_i(t_{k+1} - q_i(t_k)}{\Delta t}] + W = 0 \tag{9}$$

$$E_{potential} = \sum_{a=1}^{n} E_a^s + \sum_{b=1}^{n} E_b^b \tag{10}$$

III. RESULTS

Figure 4 and Figure 5 show the shape of catapult structure and projectile position with time. The plots are made for the center node of the string, which is pulled backward and downwards pull to reach a certain energy required for the projectile range of 10m.

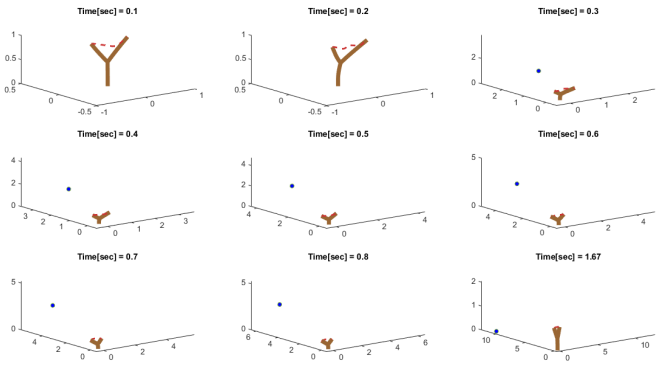

Fig. 4. Shape of Structure and Projectile position vs Time

To optimize the range of the catapult, we conducted a parametric study. The geometric and material parameters of the catapult and string are listed below in Table 1. Unless otherwise stated, the base parameter values for each

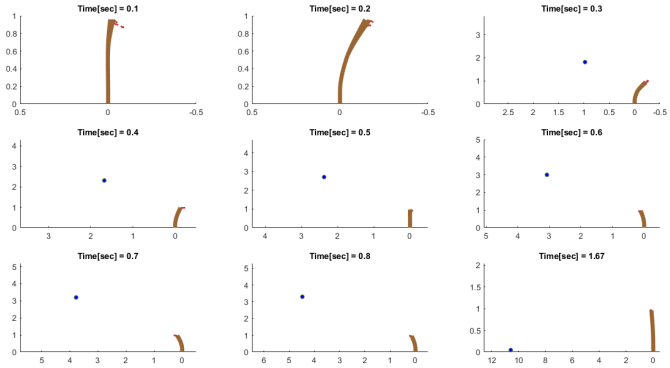

Fig. 5. Shape of Structure and Projectile position vs Time (Side View)

Parameter (units)	Variable Name	Value
catapult frame radius (m)	r_c	0.004
string radius (m)	r_s	0.01
catapult Y-angle (deg.)	α	80
catapult height (m)	h_c	1.1
catapult elastic modulus (GPa)	E_c	5×10^9
string elastic modulus (GPa)	E_s	0.005×10^9
projectile mass (kg)	m_p	0.2
launch angle (deg.)	θ	45
backward displacement (m)	δ	0.3

TABLE I

BASE PARAMETERS FOR PARAMETRIC STUDY.

parametric study are equal to the values in the table.

Due to a large number of independent variables, it is computationally inefficient to conduct a parametric optimization involving all or multiple of the variables. Thus a separate analysis will be conducted for each variable, in which its effect on the range of the projectile will be studied empirically.

Below are two 3-variable plots illustrating the relationship between catapult elastic modulus E_c, string elastic modulus E_s, and range R. The first plot is for a projectile mass $m_p = 0.1kg$, while the latter is for $m_p = 0.6kg$. In this specific analysis, the string radius is $r_c = 0.004m$.

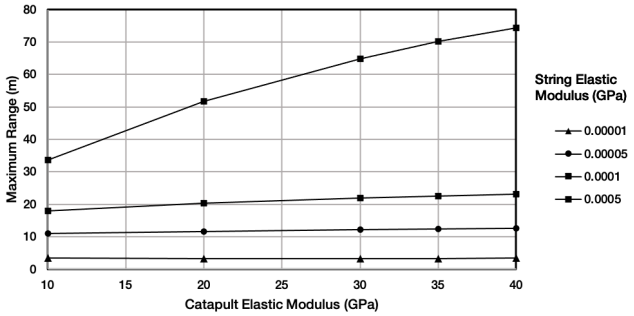

Fig. 6. Relationship between the catapult elastic modulus E_c, string elastic modulus E_s, and range y_{max} for projectile mass $m_p = 0.1kg$

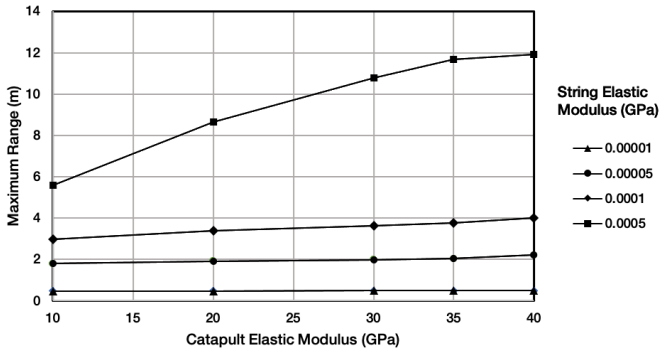

Fig. 7. Relationship between the catapult elastic modulus E_c, string elastic modulus E_s, and range y_{max} for projectile mass $m_p = 0.6kg$

As the elastic modulus of catapult increases, the range of catapult increases with diminishing returns. This effect is more pronounced with higher string elastic modulus. Increasing the string elastic modulus also increases the range exponentially. This behavior is expected because a higher elastic modulus indicates that a material can store greater amounts of elastic potential energy, which allows more energy to be transferred to the projectile and thus producing higher range. The relationship between elastic modulus E and elastic energy U is

$$U = \frac{1}{2}E\epsilon^2$$

so $U \propto E$ for linearly elastic materials. When the elastic energy of the catapult is transferred to the projectile as kinetic energy, the energy equation becomes

$$U = \frac{1}{2}mv_0^2$$

so $U \propto v_0^2$. From the kinematics equation

$$R = \frac{v_0^2 sin(2\theta)}{g}$$

the range R follows the proportionality $R \propto v_0^2 sin(2\theta)$. Thus $E \propto \frac{R}{sin(2\theta)}$. Because the release angle θ is constant at $45°$, indicating that E varies linearly with R. The results shown in Fig. 1 and Fig. 2 validate these proportionalities, with the exception of slightly diminishing increase of range for higher elastic string moduli. This may be due to the fact that the string is not truly "linearly elastic."

The inverse calculation of R was also achieved by our program, in which the target range was defined, and the backward displacement of the catapult is calculated via projectile kinematics and the energy equation $E = \frac{1}{2}mv^2$. The kinetic energy of the projectile is equated to the total elastic energy of the catapult-string system, which is then used to determine the amount, catapult must displace to acquire the required launch energy. The backward displacement is measured from the center node of the string. Note that because the angle of launch is fixed at $\theta = 45°$, the free end of catapult is also displaced *downward* by the same amount. The subsequent figure depicts the relationship between the target range and the required backward displacement of catapult.

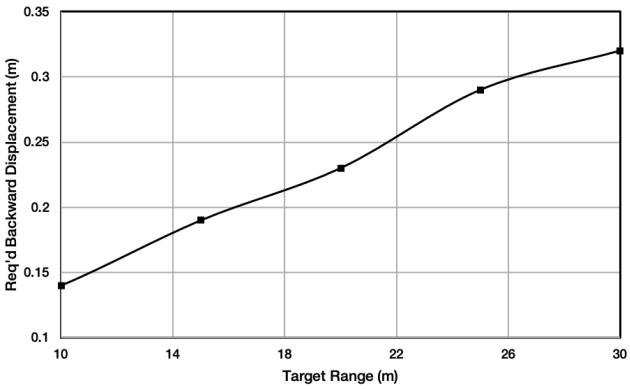

Fig. 8. Backward Displacement of string vs Target Range

The relationship between target range and backward displacement is linear in nature; as the displacement of catapult is increases, the range also increases. The relationship is approximated by $\delta = 0.0091R + 0.0527$, where δ is the required backward displacement of catapult in meters and R is the range in meters.

In the subsequent phase, parametric study and geometric parameters of the catapult are systematically manipulated. The following figure elucidates the correlation between catapult's height and resultant range of the launched projectile.

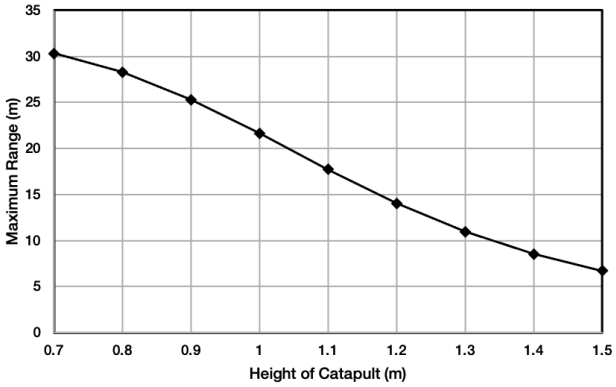

Fig. 9. Maximum Range vs Height of Catapult for a given string displacement

Based on Fig. 4, increasing the height of catapult decreases its range. The relationship is mostly linear and can be approximated by $R = -31.63h_c + 52.97$, where h_c is the catapult height. The following figure depicts the relationship between the angle of catapult y-joint and the range. Simultaneously, the length of string changes as the Y-angle is changed, but there is an efficient method to decouple these two variables.

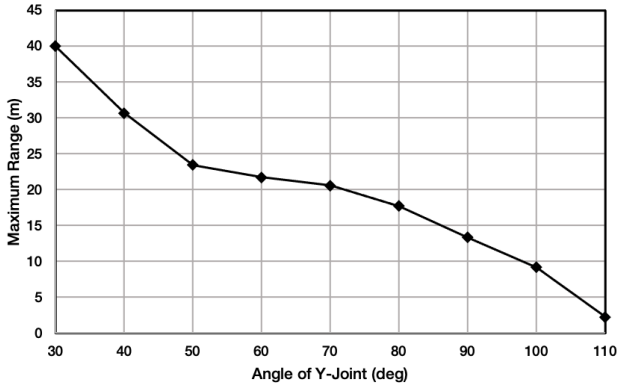

Fig. 10. Maximum Range vs Angle of Y joint

Overall increasing the angle of the Y-joint decreases the maximum range of projectile, albeit non-linearly. At increasingly acute and obtuse angles, the range deceases at a higher rate. However, increasing the angle past 110 degrees or decreasing the angle past 30 degrees causes the simulation to diverge.

The subsequent phase of the parametric analysis focuses on the radii of the catapult and the string. Figures 6 depicts the relationship between the radius of catapult frame r_c (the cross section of the catapult is hollow and circular) and the range of catapult. The inner radius of the catapult frame is 0.003m hence the simulation begins at $r_c = 0.004$m.

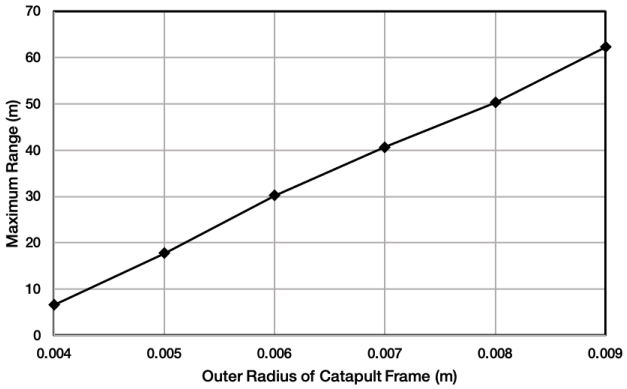

Fig. 11. Maximum Range vs Outer Radius of Catapult Frame

According to the results, range increases linearly with outer radius of the catapult frame. The linearity can be approximated by the equation $R = 11058r_c + 37.26$, where R and r_c are both in meters. A similar relationship is observed between radius of the string and the range.

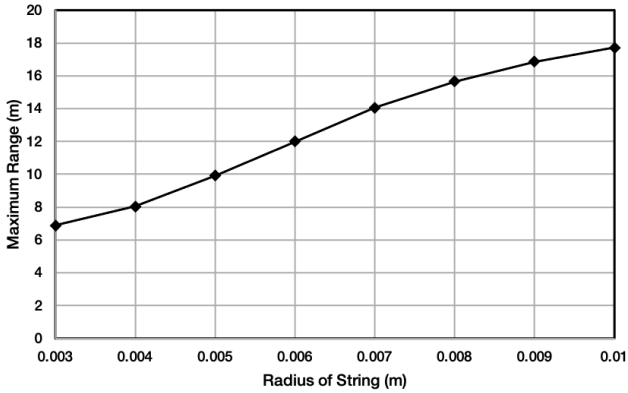

Fig. 12. Maximum Range vs Radius of String

Increasing the radius of string r_s also increases the range proportionally. The relationship can be approximated by $R = 1655.9r_s + 1.88$. This positive linear relationship is valid because the internal energy of beam increases with cross-sectional area. The governing equation for the internal energy of a Euler-Bernoulli beam with constant cross-sectional area A is

$$U = \frac{A}{2} \int_V \sigma_{xx} \delta u_x' dx$$

where σ_{xx} is the axial stress of beam and $\delta u_x'$ is the axial strain of beam. Although Euler-Bernoulli theory is a gross simplification of our catapult system, it suffices to show that the internal energy U of the system increases with the beam cross sectional area.

Overall the parametric study yields interesting insight into the mechanics of elastic structures. We observe a positive, mostly linear relationship between elastic, modulus of the string and catapult, and maximum range of the catapult. This is validated by classical theory, which dictates that internal energy of the catapult is proportional to the range of projectile. There is also a positive linear relationship between the range and required backward displacement of the catapult.

Varying the geometric parameters of the system also yielded fascinating results. Increasing height of the catapult and angle of the Y-joint decreases the maximum possible range of projectile. On the other hand, increasing the radius of catapult and string increased the range linear. The positive relationship between cross sectional area is validated by Euler-Bernoulli beam theory.

IV. Conclusion

The study has revealed a lot of insights regarding the relationships between different variables of the Y catapult on the range. Through this simulation, we have established the fact that with an increase in elastic moduli for the catapult and string, the amount of potential energy increases

which results in longer range values for a given catapult displacement. Additionally, there was a steeper increase in the elastic energy with the increase of elastic moduli. These results are of paramount importance in terms of mechanical design of the catapult. The linear relationship between the string displacement and range is another crucial observation which aligns with the natural intuition. In conclusion, the simulation model fared well with the practical aspects as the expected outcomes were observed.

REFERENCES

[1] Khera K, et al. "Design and Manufacturing of a Simple Catapult." International Press Corporation. vol 4, No 6, Dec. 2014. Accessed 5 Nov. 2023

[2] Maggiorini, Dario, et al. "Unifying Rigid and Soft Bodies Representation: The Sulfur Physics Engine." International Journal of Computer Games Technology, vol. 2014, 2014, pp. 1–12

[3] Armanini, C., et al. "From the Elastica Compass to the Elastica Catapult: An Essay on the Mechanics of Soft Robot Arm." Proceedings of the Royal Society A: Mathematical, Physical and Engineering Sciences, vol. 473, no. 2198, Feb. 2017, p. 20160870, https://doi.org/10.1098/rspa.2016.0870.

[4] Bergou, M., Wardetzky, M., Robinson, S., Audoly, B. and Grinspun, E., 2008. Discrete elastic rods. In ACM SIGGRAPH 2008 papers (pp. 1-12).

[5] K. Jawed, "Discretized Structures Notes." Structures Computer Interaction Lab. 2023.